

Poly(L-lysine)-grafted-poly(ethylene glycol)-based surface-chemical gradients. Preparation, characterization, and first applications

Sara Morgenthaler and Christian Zink

Laboratory for Surface Science and Technology, Department of Materials, ETH Zurich, Wolfgang-Pauli-Strasse 10, CH-8093 Zurich, Switzerland

Brigitte Städler and Janos Vörös

Laboratory of Biosensors and Bioelectronics, Institute for Biomedical Engineering, Department of Information Technology and Electrical Engineering, ETH Zurich, Gloriastrasse 35, CH-8092 Zurich, Switzerland

Seunghwan Lee, Nicholas D. Spencer,^{a)} and Samuele G. P. Tosatti

Laboratory for Surface Science and Technology, Department of Materials, ETH Zurich, Wolfgang-Pauli-Strasse 10, CH-8093 Zurich, Switzerland

(Received 16 October 2006; accepted 11 December 2006; published 31 January 2007)

A simple dipping process has been used to prepare PEGylated surface gradients from the polycationic polymer poly(L-lysine), grafted with poly(ethylene glycol) (PLL-g-PEG), on metal oxide substrates, such as TiO₂ and Nb₂O₅. PLL-g-PEG coverage gradients were prepared during an initial, controlled immersion and characterized with variable angle spectroscopic ellipsometry and x-ray photoelectron spectroscopy. Gradients with a linear change in thickness and coverage were generated by the use of an immersion program based on an exponential function. These single-component gradients were used to study the adsorption of proteins of different sizes and shapes, namely, albumin, immunoglobulin G, and fibrinogen. The authors have shown that the density and size of defects in the PLL-g-PEG adlayer determine the amount of protein that is adsorbed at a certain adlayer thickness. In a second step, single-component gradients of functionalized PLL-g-PEG were backfilled with nonfunctionalized PLL-g-PEG to generate two-component gradients containing functional groups, such as biotin, in a protein-resistant background. Such gradients were combined with a patterning technique to generate individually addressable spots on a gradient surface. The surfaces generated in this way show promise as a useful and versatile biochemical screening tool and could readily be incorporated into a method for studying the behavior of cells on functionalized surfaces. © 2006 American Vacuum Society.

[DOI: 10.1116/1.2431704]

I. INTRODUCTION

Controlling the processes regulating the spontaneous adsorption of biomolecules onto artificial material surfaces is a critical consideration when designing and developing modern biomedical and bioanalytical devices.^{1–4} Surfaces such as polymers and metal oxides, which are widely used in the biomaterials area, have indeed been shown to nonselectively adsorb large quantities of proteins in their native state. For applications in areas such as tissue engineering, implants, or biosensors, those surfaces need to be rendered “protein resistant,” which means resistant towards nonspecific protein adsorption to minimize nonspecific biological response. Common features of nonfouling (i.e., protein-resistant) surfaces are their hydrophilicity, their charge neutrality, as well as the presence of hydrogen bond acceptors, but absence of hydrogen bond donor groups.⁵

Several ways to create protein-resistant surfaces have been proposed: poly(ethylene glycol) chemistry,^{2,5,6} functionalized alkanethiols,^{7–9} supported phospholipid bilayers,^{10,11} polysaccharide chemistry,^{12–15} and others.

Among them, the most popular approach is based on the use of poly(ethylene glycol) (PEG). The protein resistance of PEG modified surfaces is attributed mainly to entropic repulsion and the high water content of the PEG chains. Among other methods, PEG chains may be immobilized on surfaces via covalent coupling, either by “grafting to,”^{16–19} or “grafting from,”²⁰ via the adsorption of PEG-containing block copolymers,^{18,21–23} graft copolymers,^{24,25} and interpenetrating polymer networks^{26,27} and via functionalization with ethylene glycol-terminated alkanethiols^{7,28–31} or silanes.^{32,33} For the platforms dealing with PEG in a brushlike conformation, it was found that the most important parameter determining the protein resistance is the ethylene glycol monomer density on the surface n_{EG} expressed as EG units/surface unit.³⁴

We have used the graft copolymer poly(L-lysine)-graft-poly(ethylene glycol) (PLL-g-PEG), because the latter system has several advantages over other PEG-based approaches [Fig. 1(a)].²⁴ The positively charged PLL backbone adsorbs electrostatically from an aqueous solution onto negatively charged surfaces, such as TiO₂ or Nb₂O₅, and the grafted PEG chains render these surfaces resistant towards nonspecific protein adsorption.^{24,35} The architecture of the

^{a)}Author to whom correspondence should be addressed; electronic mail: spencer@mat.ethz.ch

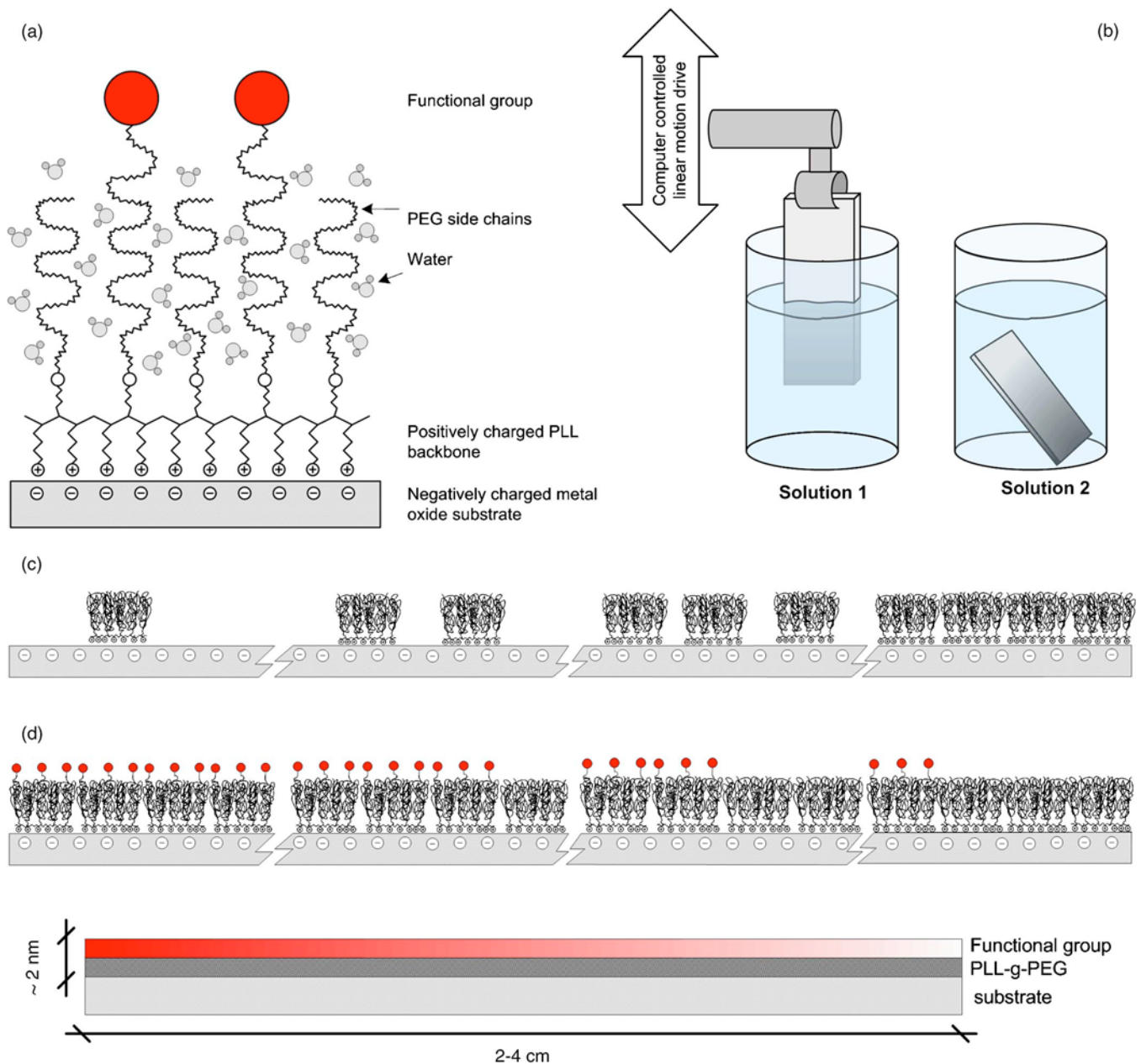


FIG. 1. (a) Schematic view of a poly(L-lysine)-grafted-poly(ethylene glycol) (PLL-g-PEG/PEG-X) adlayer on a metal oxide surface. The positively charged PLL backbone attaches to the negatively charged metal oxide layer through electrostatic interactions. The grafted PEG chains are hydrated (represented by the H_2O molecules between the PEG chains) and extend into the aqueous environment (reproduced with permission from Tosatti *et al.*). (b) Schematic of the gradient preparation process. Gradients are prepared in two steps, a gradual immersion into one type of solution, followed by a full immersion into a second type of solution. Schematic of the two gradients prepared in this study: (c) PLL-g-PEG coverage gradient after a single immersion step (PLL-g-PEG on bare $\text{TiO}_2/\text{Nb}_2\text{O}_5$) and (d) functionalized PLL-g-PEG gradient after two immersion steps (PLL-g-PEG/PLL-g-PEG/PEG-biotin).

graft copolymer (molecular weight of the PEG chains and grafting ratio) and the adsorbed mass determine the ethylene glycol density on the surface.^{34,36,37} Serum adsorption was found to decrease below the detection limit of optical waveguide lightmode spectroscopy (OWLS) measurements for ethylene glycol densities $\geq 20 \text{ nm}^{-2}$.³⁴ Specific (bio)functional groups can be attached at the ω position of the PEG side chains, e.g., biotin,³⁸ nitrilotriacetic acid,³⁹ or bioadhesive peptides such as Arg-Gly-Asp (RGD),^{40,41} resulting in a surface that exposes a specific functionality in a protein-resistant background. In all those examples the degree of

functionalization is of crucial importance when looking for optimal antibody immobilization³⁸ or cell response.⁴²

Since a screening process is often expensive in terms of time and material, a surface gradient with a gradually changing antigen or receptor density can contribute to improving selection processes while screening a large range of properties on one single sample under the same experimental conditions. Additionally, since gradients are found to play a key role in understanding biological processes such as the growth of nerve cells, fabricated surface (bio)chemical gradients may be a powerful experimental tool to further investigate

these mechanisms.⁴³ A variety of techniques to generate grafted polymer gradients is available, including the preparation of initiator gradients by corona discharge,^{44,45} by vapor diffusion,^{46,47} by controlling adsorption kinetics⁴⁸ or temperature,⁴⁹ the control of the polymerization conditions, e.g., time^{50,51} or temperature,⁵² and diffusion methods.^{53,54} Some of these surfaces have been used to study cell growth. Other techniques have been used to gradually immobilize biomolecules, such as proteins, on surfaces, for example, microfluidics,^{55–57} covalent coupling to an alkanethiol gradient,^{58,59} covalent coupling by laser irradiation,⁶⁰ the use of stamping techniques and electrophoretics,⁶¹ ink-jet printing,^{62,63} drainage,⁶⁴ or by controlling the adsorption kinetics.⁶⁵

In this study we present the generation and characterization of PLL-*g*-PEG gradients prepared by means of an immersion process originally developed for alkanethiols [Fig. 1(b)].⁶⁶ Two different types of PLL-*g*-PEG gradients with either nonfunctionalized [Fig. 1(c)] or biotinylated PEG chains [Fig. 1(d)] were prepared on titanium and niobium oxide surfaces, respectively, and characterized by means of variable angle spectroscopic ellipsometry (VASE) and x-ray photoelectron spectroscopy (XPS).

The gradients on TiO₂ were used to investigate the influence of PLL-*g*-PEG surface coverage, i.e., ethylene glycol density, on the adsorption behavior of different proteins that are relevant in terms of their occurrence and role in blood functions and wound healing processes, namely, human serum albumin, fibrinogen, and immunoglobulin G, and mixed protein solutions, such as blood serum and blood plasma. Since TiO₂ is a widely used implant material, a detailed knowledge of protein interaction with this surface is of great importance and gradient techniques should allow one to determine the minimum EG monomer surface density needed to prevent protein adsorption for a certain type of protein.⁶⁷ Additionally, the streptavidin/biotin interaction was monitored with biotinylated gradients by confocal laser scanning microscopy. These gradients were then combined with an in-house patterning technique termed molecular assembly patterning by lift-off (MAPL),⁶⁸ which creates micropatterned surfaces of functionalized spots in a protein-resistant background of PLL-*g*-PEG. A simple combination of gradients with a patterning technique offers the possibility for a quantitative comparison of different samples, as the protein-resistant background of the pattern enables us to calibrate the measurements. The gradual change in active-group concentration in successive patches makes these gradients interesting tools, likely to find manifold applications in the areas of biosensors or cell studies.

II. EXPERIMENTAL SECTION

A. Materials

All adsorption experiments were carried out from a “HEPES 2” buffer consisting of 10 mM 4-(2-hydroxyethyl)piperazine-1-ethane-sulfonic acid and 150 mM NaCl (both from MicroSelect, Fluka Chemie GmbH, Switzerland)

in ultrapure water [MilliQ gradient A 10 system, resistance $\approx 18 \text{ M}\Omega/\text{cm}$, total organic carbon < 4 ppb (parts per 10⁹), Millipore Corporation, USA]. The buffer was adjusted to pH 7.4 by the use of 6M NaOH and filtered through a 0.2 μm filter (Millex-GW, Millipore, Switzerland) prior to use.

PLL-*g*-PEG, a graft copolymer with a PLL backbone of 20 kDa, (including counterions, Br⁻), PEG side chains of 2 kDa, and a grafting ratio of 3.5, was used for all experiments. The biotinylated polymer (PLL-*g*-PEG/PEG-biotin) had the same architecture, with 50% of its side chains biotinylated using PEG-biotin of 3.4 kDa. Both polymers were synthesized and characterized as previously described in detail.^{34,38} Briefly, a 100 mM solution of PLL-HBr (Fluka, Switzerland) in 50 mM sodium tetraborate buffer (pH 8.5) was prepared and filter sterilized (0.22 μm pore size filter, Millex, Sigma-Aldrich, Switzerland). The grafting reaction was carried out by adding *N*-hydroxysuccinimidyl ester of methoxypoly(ethylene glycol) propionic acid (Nektar, USA) and allowing to react for 6 h at room temperature. Subsequently, the reaction mixture was dialyzed (Spectra-Por, molecular weight cutoff size of 6–8 kDa, Spectrum Laboratories Inc., USA) for 48 h against de-ionized water. The grafting ratio of the polymer was determined by ¹H NMR. The product was freeze dried and stored at $-20 \text{ }^\circ\text{C}$ before use. Human serum albumin [molecular weight (MW) = 66.4 kDa], rabbit Immunoglobulin G (IgG) (MW = 150 kDa), fibrinogen (MW = 340 kDa, all from Sigma Aldrich Chemie GmbH, Germany), blood serum (Precinorm U, Roche, Switzerland), and fresh frozen plasma were used for the protein-adsorption studies. Streptavidin alexa fluor488 (MW = 52.8 kDa, Invitrogen, Switzerland) was used for confocal laser scanning microscopy.

B. Substrates

TiO₂ and Nb₂O₅ thin films (15 nm) were sputter coated onto silicon wafers (WaferNet GmbH, Germany) and Nb₂O₅ (6 nm) onto Pyrex wafers (SensorPrep Services, USA) using reactive magnetron sputtering (PSI Villigen, Switzerland). Prior to use, the oxide-coated substrates were cleaned by the following protocol: (i) 10 min sonication in 2-propanol and (ii) 2 min oxygen-plasma cleaning in a plasma cleaner/sterilizer PDC-32G instrument (Harrick, Ossining, NY, USA). The Nb₂O₅ coated Pyrex substrates were prepatterned with photoresist (S1818, Shipley, USA) according to the procedure described by Falconnet *et al.*⁶⁸ Finally, these samples were sonicated in water for 10 min and plasma cleaned for 5 s in an oxygen plasma prior to functionalization.

C. Surface modification

Gradients were prepared based on a procedure adapted from Morgenthaler *et al.*⁶⁶ The PLL-*g*-PEG was gradually adsorbed onto an oxide surface by an immersion process. A concentration of 0.02 mg/ml PLL-*g*-PEG in HEPES 2 and a total immersion time of 17 min were used. The substrate was dipped gradually with a linear motion drive (OWIS GmbH, Germany), according to a stepwise immersion program

(LABVIEW software V7.1, National Instruments). After this gradual coating step the substrates were rinsed immediately with HEPES 2 and ultrapure water and dried under a nitrogen stream. When biotinylated gradients were prepared, the gradual coating step was performed in a 0.02 mg/ml PLL-g-PEG/PEG-biotin solution with the same immersion program. After rinsing and drying the substrate was backfilled with nonfunctionalized PLL-g-PEG (0.1 mg/ml) for 40 min.

As references, homogeneously coated surfaces were prepared according to a previously published protocol³⁴ and bare, oxide-coated surfaces were immersed in HEPES 2 for 17 min.

D. Protein adsorption

All single proteins were adsorbed from a 0.1 mg/ml solution in HEPES 2. Gradient and reference samples were exposed to the protein solution for 15 min, then subjected to rinsing with HEPES 2 and ultrapure water, and finally dried under a stream of nitrogen. Serum and plasma were used as received without further dilution. Variable angle spectroscopic ellipsometry measurements were carried out in a dry state.

E. Variable angle spectroscopic ellipsometry (VASE)

The dry thicknesses of polymer and protein adlayers were determined by VASE (M-2000F, L.O.T. Oriel GmbH, Germany). Measurements were conducted under ambient conditions at three angles of incidence (65°, 70°, and 75°) in the spectral range of 370–1000 nm. Spectroscopic scans were taken after every step (after cleaning, after PLL-g-PEG adsorption, and after protein adsorption) every 3 or 5 mm along the sample. Three samples were analyzed for each type of protein. Measurements were fitted with the WVASE32 analysis software using a multilayer model for an oxide layer on silicon and an organic adlayer (polymer and protein). The n and k values for the oxide layers were fitted, and the adlayer thickness for both the PLL-g-PEG and the proteins was determined using a Cauchy model ($A=1.45$, $B=0.01$, and $C=0$).²³

F. X-ray photoelectron spectroscopy (XPS)

XPS analysis was performed using a VG Theta Probe spectrophotometer (Thermo Electron Corporation, West Sussex, UK) equipped with a concentric hemispherical analyzer and a two-dimensional channel plate detector with 112 energy and 96 angle channels and a total aperture of 60°. Spectra at 10 or 20 different locations on the gradient sample (line scan with a point-to-point analysis spacing of 3.4 or 1.7 mm, respectively) were acquired at a base pressure of 10^{-9} mbar or below using a monochromatic Al $K\alpha$ source with a spot size of 300 μm . The measurements were repeated three times for each type of gradient. The instrument was run in the standard lens mode at 53° to the surface normal for survey spectra and in an eight-angle-channel mode for detailed spectra, each channel covering a sector of 7.5° and having the most grazing angle at 79.25° from the surface normal.

The analyzer was used in the constant analyzer energy mode. Pass energies used for survey scans and detailed scans were 200 and 150 eV, respectively, for titanium Ti $2p$, carbon C $1s$, oxygen O $1s$, and nitrogen N $1s$. Acquisition times were approximately 30 min in total for high-energy-resolution elemental scans and 5 min for survey scans. These experimental conditions were chosen to obtain an adequate signal-to-noise ratio in a minimum time and to limit beam-induced damage. Under these conditions, sample damage was negligible, and reproducible analyzing conditions were obtained on all samples. All recorded spectra were referenced to the hydrocarbon C $1s$ signal at 285.0 eV. Data were analyzed using the program CASAXPS (Version 2.3.5, www.casaxps.com).

The signals were fitted using Gaussian-Lorentzian functions and least-squares-fit routines following a Shirley iterative background subtraction according to the protocol published by Huang *et al.*³⁵

The different intensity ratios have been calculated by dividing the corresponding areas underneath the spectra. Since the main aim of the XPS measurements was to observe trends along the gradient, sensitivity factors were not employed.

G. Molecular assembly patterning by lift-off (MAPL)

The MAPL technique was applied to Nb₂O₅ coated Pyrex wafers (Sensor Prep Services, USA) as described by Falconet *et al.*⁶⁸ Briefly, photolithography was used to create substrates with a patterned photoresist coating. After coating the prepatterned substrate with PLL-g-PEG/PEG-biotin in a concentration gradient, the photoresist was lifted off in 1-methyl-2-pyrrolidone [peptide-synthesis grade ($\geq 99.5\%$), Fluka Chemie GmbH, Switzerland]. Subsequently, the uncovered background was backfilled with nonfunctionalized PLL-g-PEG (0.1 mg/ml). The sample was placed in a polydimethylsiloxane-based flow cell (12 mm in length) and rinsed with buffer solution. The buffer solution was replaced with streptavidin alexa fluor488 (20 $\mu\text{g}/\text{ml}$) for 40 min. After rinsing with buffer, the sample was investigated using a confocal laser scanning microscope (Zeiss LSM 510, Germany) equipped with a 10 \times objective (0.3 numerical aperture Ph1 Plan-Neofluar, Zeiss, Germany), an argon laser, and the required filter sets. All images were taken with exactly the same instrument settings, allowing for a quantitative comparison.

H. Optical waveguide lightmode spectroscopy (OWLS)

OWLS measurements were carried out in OWLS 110 instruments (MicroVacuum, Hungary) using a laminar flow-through cell ($8 \times 2 \times 1 \text{ mm}^3$). The formula of Defeijter *et al.* was applied to calculate the adsorbed mass⁶⁹ with a refractive index increment (dn/dc) of 0.139 cm^3/g for PLL-g-PEG and 0.182 cm^3/g for proteins.³⁸ The adsorbed mass was further converted into EG monomer surface density according to Pasche *et al.*³⁴ Waveguides were initially placed in the buffer immediately after the cleaning and allowed to soak

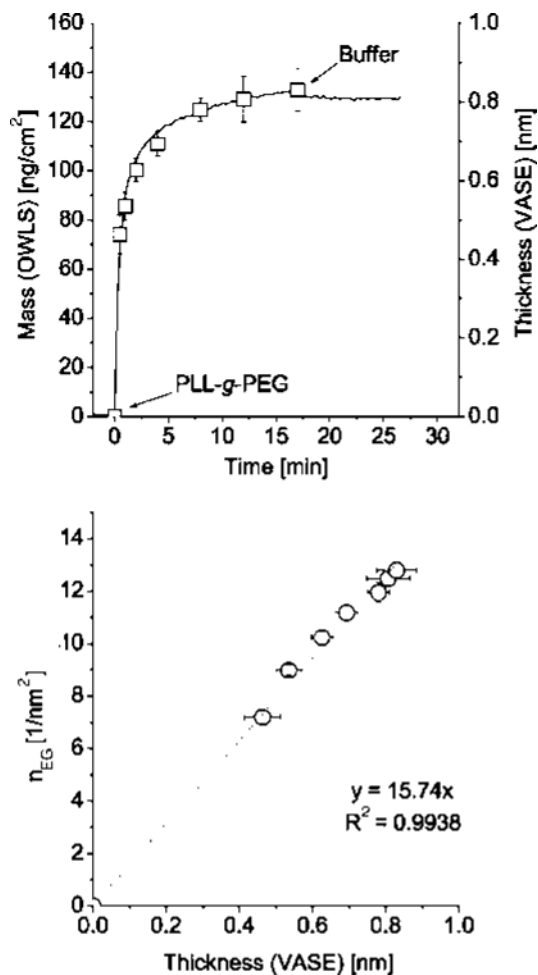


FIG. 2. Upper panel: adsorption kinetics for a 0.02 mg/ml PLL-g-PEG solution in HEPES 2 as measured by OWLS (adsorbed mass vs time, line) and VASE (layer thickness vs time, \square). 17 min is needed to reach a plateau value in the adsorption curve. Lower panel: direct comparison of layer thickness from VASE and EG monomer surface density derived from OWLS measurements for different adsorption times. A good correlation was found between both techniques, allowing for a conversion of adsorbed thickness into EG monomer surface density n_{EG} .

overnight. The samples were exposed *in situ* to the PLL-g-PEG solution at a concentration of 0.02 mg/ml. The adsorption was subsequently monitored for 17 min. Then, the polymer solution was replaced with buffer. Next the PLL-g-PEG modified samples were exposed to full human serum for 15 min before rinsing again with buffer solution.

III. RESULTS AND DISCUSSION

A. Gradient preparation

The gradient-preparation method used was based on controlling the adsorption kinetics. OWLS measurements were applied to determine the adsorption kinetics for different PLL-g-PEG concentrations (data not shown). For all concentrations a fast initial adsorption step was observed, followed by slow surface rearrangements that allow the adsorption of more polymer.²⁴ Huang *et al.* found that for a concentration of 1 mg/ml, 95% of the adlayer is formed in the first 5 min

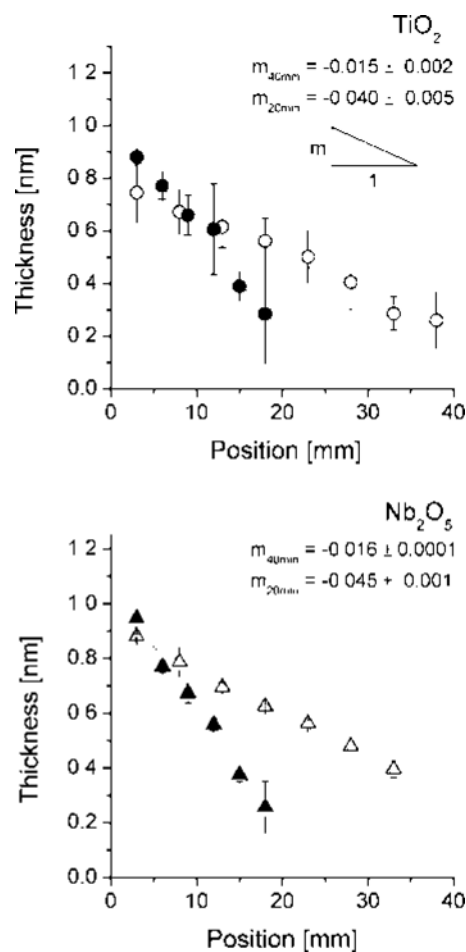


FIG. 3. Thickness of the adsorbed polymer adlayer measured by VASE as a function of position for different gradients. Upper panel: 20-mm-long (\bullet , $R^2 = -0.9973$) and 40-mm-long (\circ , $R^2 = -0.9908$) gradients on TiO₂ substrates; lower panel: 20-mm-long (\blacktriangle , $R^2 = -0.9981$) and 40-mm-long (\triangle , $R^2 = -0.9966$) gradients on Nb₂O₅ substrates. A linear increase in thickness was found for all types of gradients (see R^2 values). Similar slopes (similar m values) are obtained for the same length on both oxide substrates (both 40-mm- and 20-mm-long gradients were prepared by the same immersion program).

of the adsorption, while it takes 20 min to reach saturation.³⁵ The time needed to form a complete adlayer increases as the concentration of the solution decreases. We determined, by means of OWLS, that for a concentration of 0.02 mg/ml PLL-g-PEG, the saturation level is reached after an immersion time of 17 min (Fig. 2, upper panel). Serum adsorption was reduced by 99% compared to a bare TiO₂ coated substrate on such a coating (data not shown). This is in spite of the relatively low density of the PLL-g-PEG layer generated from the 0.02 mg/ml solution ($7.8 \pm 0.4 \text{ \AA}$). For comparison, a layer formed from 1 mg/ml solution for 30 min is $11.7 \pm 0.4 \text{ \AA}$ in thickness. The lower panel in Fig. 2 shows the correlation between EG monomer surface density, n_{EG} , derived from OWLS and adlayer thickness from VASE measurements for identical adsorption times. The correlation of these data allowed us to switch between the two methods using the conversion factor obtained by linear regression.

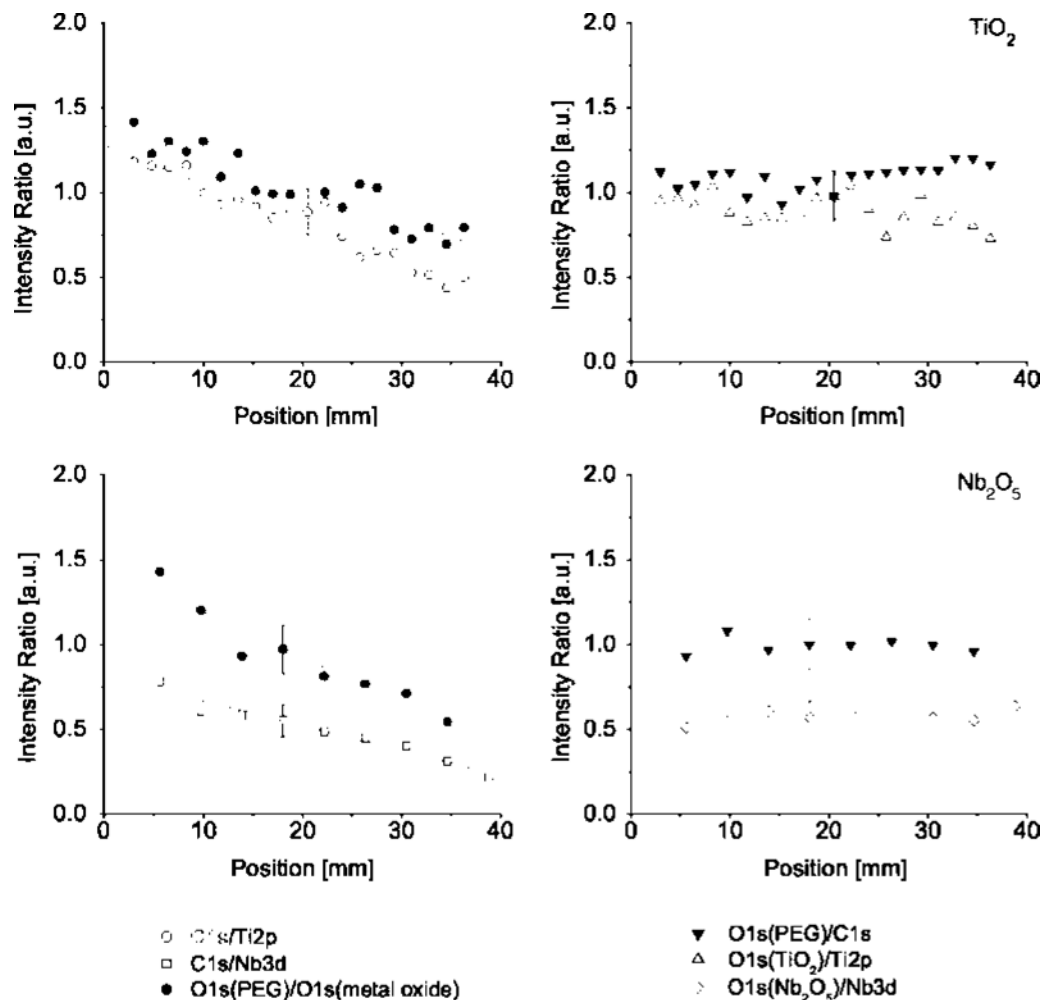


FIG. 4. Intensity ratios measured by XPS at 79.25° takeoff angle as a function of position for 40 mm gradients on TiO₂ (upper panel) and Nb₂O₅ (lower panel) substrates. Left column: both ratios that are sensitive to the surface coverage (C 1s/metal oxide) and O 1s (PEG)/O 1s (metal oxide) indicate the presence of a linear gradient composition [C 1s/Ti 2p: $R^2 = -0.97$, O 1s (PEG)/O 1s (TiO₂): $R^2 = -0.92$, C 1s/Nb 3d: $R^2 = -0.98$, and O 1s (PEG)/O 1s (Nb₂O₅): $R^2 = -0.96$], while the ratios relative to the composition of the substrate [O 1s (metal oxide)/metal oxide] or the adlayer [O 1s (PEG)/C 1s] remain constant (right column) as function of the position.

We observed that when a substrate is immersed at a constant speed for 17 min (for example, at 40 $\mu\text{m/s}$ for a 4-cm-long sample), a nonlinear coverage gradient is formed, corresponding to the shape of the adsorption curve as measured by OWLS (Fig. 2, upper panel). The immersion program was therefore modified to generate a linear coverage gradient by gradually changing the immersion speed by means of a program based on an exponential function. This gradient preparation method was used to generate two types of gradients: PLL-*g*-PEG coverage gradients on bare oxide surfaces [Fig. 1(b)] and functionalized PLL-*g*-PEG/PEG-biotin gradients [Fig. 1(c)].

B. PLL-*g*-PEG versus oxide gradients

One-component PLL-*g*-PEG gradients were obtained by the immersion of either a TiO₂ or a Nb₂O₅ coated substrate according to a nonlinear speed program. Figure 3 presents the results obtained by means of variable angle spectroscopic ellipsometry for 20- and 40-mm-long gradients on TiO₂ (upper panel) and Nb₂O₅ (lower panel) substrates. The same

immersion program was used for both oxide substrates, which leads to a very similar slope, indicating that the adsorption kinetics on both substrates are comparable. A linear increase in adlayer thickness can be found for all types of gradients (all R^2 values are higher than -0.99). Grazing-angle x-ray photoelectron spectroscopy measurements were also performed on such gradients (Fig. 4). We expect that the adlayer surface coverage decreases with decreasing immersion time (expressed as position on the gradient). One parameter that is highly sensitive to variations in the adlayer film thickness is the carbon/metal ratio, since these elements are found either only in the adlayer (carbon) or in the substrate (metal). The same information can be obtained when considering the ratio between the O 1s (PEG) and the O 1s (metal oxide) signals (left column). Finally, the fact that both the ratios O 1s (PEG) versus carbon and O 1s (metal oxide) versus metal oxide (Ti 2p or Nb 3d) remain constant along the gradient suggests that the adsorbed adlayer consists primarily of PLL-*g*-PEG.

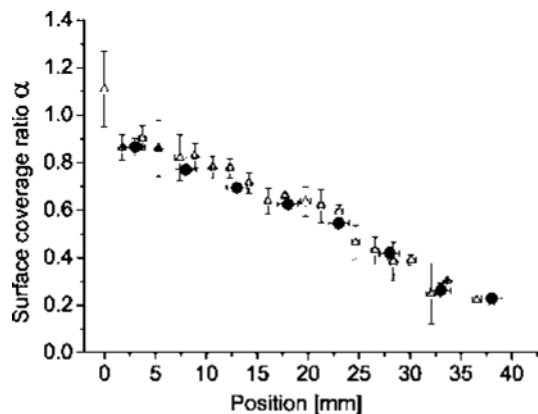


FIG. 5. Relative PLL-g-PEG surface coverage α for a single-component gradient on TiO₂ as determined by XPS (Δ) and VASE (\bullet). A bare metal oxide surface exposed to HEPES 2 (α equal to zero) and a homogeneously coated sample (α equal to 1) were used as references. The relative surface coverage α decreases continuously towards the loosely covered end. VASE and XPS measurements correlate with each other.

To further compare VASE and XPS data a surface coverage parameter α was defined as the ratio between coated and uncoated surface areas at a point X on the gradient. A bare metal oxide surface exposed to HEPES 2 (α equal to zero) and a homogeneously PLL-g-PEG-coated sample (α equal to 1) were used as references. We chose to use the C/Ti ratio measured by XPS at an angle of 79.25° normal to the surface to calculate α , since at such a grazing angle, the signals are highly surface sensitive. α is then calculated from the adlayer thickness measured by VASE and the C/Ti ratio measured by XPS at individual positions on the gradient. The results show that both relative surface coverages are found to correspond well to each other and to decrease monotonically along the substrate length with decreasing immersion time (Fig. 5). The fact that zero coverage is not reached is mostly due to the adventitious contamination that adsorbs when exposing the gradient to ambient conditions during the deposition.

C. Protein adsorption on PLL-g-PEG coverage gradients

PLL-g-PEG coverage gradients on TiO₂ were exposed to a series of different protein solutions. The thickness of the PLL-g-PEG adlayer and the adsorbed protein layer was measured with VASE under dry conditions. Figure 6 represents the relative adsorbed amount of proteins that are deposited on a PLL-g-PEG coverage gradient compared to a bare TiO₂ substrate (value=1) and a homogeneously coated substrate as a function of the ethylene glycol monomer surface density n_{EG} . The measured dry thickness of the gradient polymer adlayer was thereby converted into EG monomer surface density, as proposed above. The amount of adsorbed protein was found to decrease towards higher EG monomer surface densities, which corresponds to the more densely covered end of the gradient. Albumin, IgG, and fibrinogen adsorption all decrease to below the detection limit of ellipsometry measurements (estimated to be 5–10 ng/cm²)^{23,41} at the PLL-

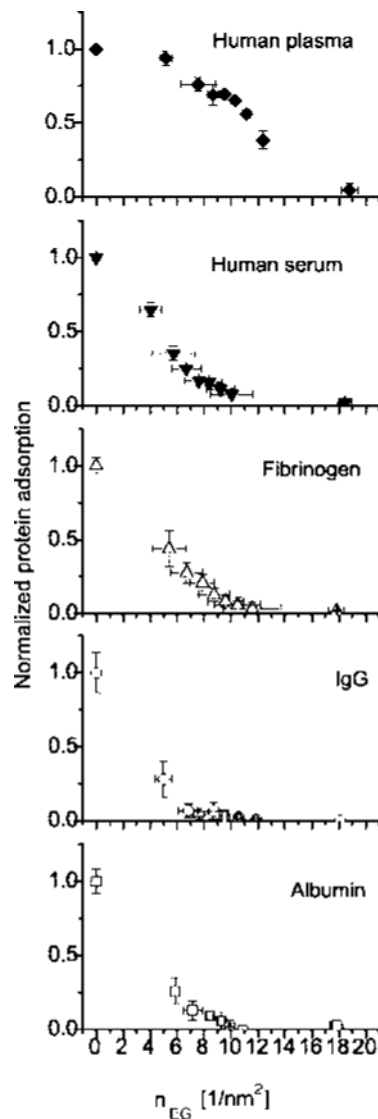


FIG. 6. Relative amount of protein adsorbed on PLL-g-PEG coverage gradients on TiO₂ plotted as a function of the EG monomer surface density, n_{EG} , calculated from OWLS/VASE adsorption data and NMR grafting ratios of the bulk polymers. The adsorbed amount of protein has been normalized by the values measured on the homogeneously coated and bare substrates. Protein adsorption is found to decrease towards the more densely covered end. The minimal PLL-g-PEG thickness at which protein adsorption is reduced to below 5% differs for each of the proteins (albumin, IgG, and fibrinogen). Mixed protein solutions, such as plasma and serum, require a higher EG monomer surface density to provide a protein-resistant coating.

g-PEG rich end as well as on the homogeneously coated substrates. However, the minimal PLL-g-PEG thickness, at which the protein adsorption falls below 5% (equals to at least a 95% reduction) in comparison with bare titanium, differs for each of the proteins: n_{EG} (IgG) ≥ 9.5 nm⁻², n_{EG} (albumin) ≥ 9.9 nm⁻², and n_{EG} (fibrinogen) ≥ 11.6 nm⁻². This may be explained by the size, shape, and charge distribution of the proteins. While albumin is a triangular protein with a small molecular weight (MW of around 66 kDa), IgG (Y shaped, MW of around 150 kDa) and fibrinogen (elongated rod, MW of around 340 kDa) are substantially larger, however, at physiological pH they are all slightly negatively

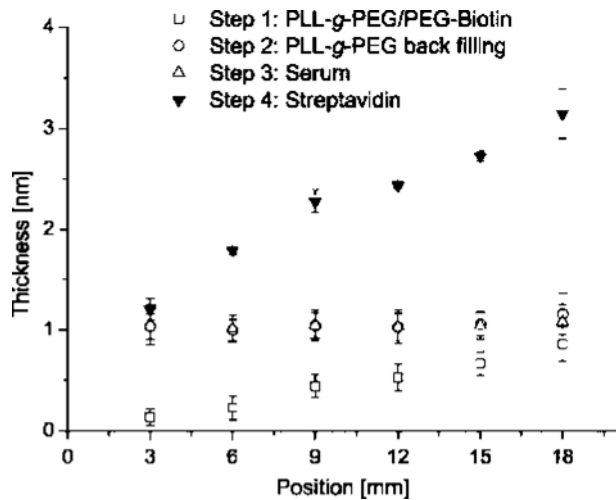


FIG. 7. Ellipsometric adlayer thickness of a biotinylated gradient as a function of the gradient position. Results are shown after four different protocol steps. A biotinylated coverage gradient was generated (step 1, linear increase in thickness), which was then backfilled with unmodified PLL-g-PEG (step 2, constant layer thickness). Negligible serum adsorption was found on such a functionalized gradient (step 3, no notable increase in layer thickness), while the amount of immobilized streptavidin gradually increased along the gradient (step 4, increasing thickness with increasing biotin density).

charged.⁵ Fibrinogen adsorbs on denser PLL-g-PEG layers because it has the possibility to attach to the substrate via various binding sites due to its elongated shape and high molecular weight.⁵ This suggests the existence of some very small uncovered patches (defects) present in the denser PLL-g-PEG that allow fibrinogen to reach the substrate-polymer interface and interact, whereas albumin and IgG need either larger or more closely spaced uncovered patches to interact with the surface, as suggested by the lower PLL-g-PEG coverage needed to reduce adsorption.

Adsorption from two mixed protein solutions, human serum and plasma, was not totally inhibited even on the high-EG-monomer-surface-density end of the gradient. Serum adsorption is reduced by 90%, whereas plasma adsorption is only reduced by 60%. There are two possible reasons, one being that both protein solutions were used at high concentrations, without further dilution. The chance for protein aggregation is higher at high concentrations. Such aggregates are less mobile than single proteins, which could possibly lead to an increased sedimentation that is difficult to remove with a short rinsing step. Another reason for the higher amount of protein adsorbed from plasma could be the presence of clotting factors, such as fibrinogen, that would lead to an increased aggregate formation.

D. PEG versus PEG-biotin gradients

Functionalized PLL-g-PEG gradients were prepared in two subsequent immersion steps, as described above. Figure 7 displays the adlayer thickness after the different steps of the protocol as a function of the position on the gradient. A one-component PLL-g-PEG/PEG-biotin gradient (Fig. 7, step 1) was backfilled with unmodified PLL-g-PEG, which gradually filled up the empty sites on the surface (Fig. 7, step

2). When exposing such a functionalized gradient to serum, a minimum adsorption (below the detection limit) was to be found all over the sample (Fig. 7, step 3), showing that the functionalized gradient coating is protein resistant. However, when the substrate was exposed to streptavidin, a gradient in adsorption along the substrate was found, being higher at the highly biotinylated end (Fig. 7, step 4). This demonstrates that the attached functional groups are active and available for specific immobilization.

E. Patterning of PLL-g-PEG/PEG-biotin gradients

Falconnet *et al.* have presented a simple method to pattern substrates by a combination of standard photolithography and molecular self-assembly termed MAPL.⁶⁸ The combination of the gradient approach with the MAPL technique allows for the generation of an array of discrete surface patches with variable bioligand concentrations along the direction of the gradient. This was demonstrated by the fabrication of a gradient of PLL-g-PEG and PLL-g-PEG/PEG-biotin on a Nb₂O₅ surface covered with prepatterned photoresist. After photoresist removal and backfilling with nonfunctionalized PLL-g-PEG, biotin-functionalized patches were created in a protein-resistant background. Such gradient patterns were visualized by adsorption of fluorescently labeled streptavidin and imaged by means of confocal laser scanning microscopy. Figure 8 depicts the fluorescence intensity of the surface-immobilized streptavidin, which decreases along the gradient when moving from the high towards the low biotin-density end of the sample. The size of the flow cell allowed us to image only 12 mm in the middle of the 20-mm-long gradient. This means that the highest measured fluorescent intensity (here set as 1) represents the most densely packed biotin spots within the flow cell but not on the full gradient, whereas the intensity at low biotin density, which corresponds to 15 mm along the gradient, is not equal to zero. Even if we lose a certain part of the information given by the gradient, it is important to use a flow cell to exchange the solutions, because drying effects, which might induce denaturation of certain proteins, would influence the outcome of our experiments. Two images taken at the extreme ends of the gradient in the flow cell are provided in addition to the fluorescence-intensity plot (at around 5 mm from the ends of the gradient). This array of discrete patches with variable biotin concentrations in a background that is resistant to streptavidin adsorption readily allows for the use of such gradients in the biosensor and molecular recognition area.

IV. CONCLUSIONS

We have presented a method to prepare chemical gradients from the polycationic graft copolymer PLL-g-PEG on oxide surfaces. First, PLL-g-PEG coverage gradients were prepared by controlling the adsorption time of the molecules during an immersion process. Single-component gradients from functionalized PLL-g-PEG may be backfilled with nonfunctionalized PLL-g-PEG to generate two-component gradients with functional groups such as biotin presented in a

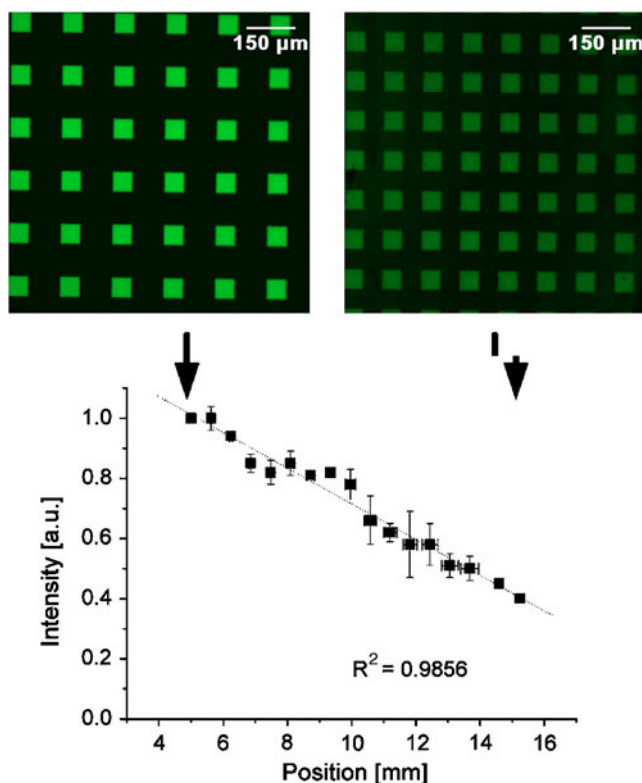


FIG. 8. Fluorescence intensity taken from confocal fluorescence microscopy images as a function of position on patterned biotinylated PLL-*g*-PEG gradients functionalized with fluorescently labeled streptavidin. The fluorescence signal decreases along the gradient, corresponding well to the trend found on unpatterned samples (Fig. 7). Images taken at a distance of 5 mm (left) and 15 mm (right) on the gradient, corresponding to both ends of the flow cell we used, are given as indicated by the arrows.

protein-resistant background. Proteins of different sizes and shapes were adsorbed onto single-component gradients. We have shown that the adsorption of smaller (albumin) and irregularly shaped (IgG) proteins can be inhibited by relatively less dense PLL-*g*-PEG layers than those required to prevent the adsorption of fibrinogen. Two-component gradients with biotinylated and nonfunctionalized PLL-*g*-PEG were also prepared and characterized. Such gradients, combined with patterning techniques, can be useful, high-throughput, and cost-effective tools in the study of biointerfaces, especially for probing the effect of bioligand concentration on specific interactions.

ACKNOWLEDGMENT

The authors acknowledge generous financial assistance for this project from the Swiss National Science Foundation.

¹W. Senaratne, L. Andruzzi, and C. K. Ober, *Biomacromolecules* **6**, 2427 (2005).

²P. Kingshott and H. J. Griesser, *Curr. Opin. Solid State Mater. Sci.* **4**, 403 (1999).

³M. Tirrell, E. Kokkoli, and M. Biesalski, *Surf. Sci.* **500**, 61 (2002).

⁴B. Kasemo, *Surf. Sci.* **500**, 656 (2002).

⁵P. Vermette and L. Meagher, *Colloids Surf., B* **28**, 153 (2003).

⁶J. M. Harris, *Poly(ethylene glycol) Chemistry and Biological Applications* (American Chemical Society, Washington, DC, 1997), Vol. 680.

⁷C. Palegrosdemange, E. S. Simon, K. L. Prime, and G. M. Whitesides, *J. Am. Chem. Soc.* **113**, 12 (1991).

⁸Y. Y. Luk, M. Kato, and M. Mrksich, *Langmuir* **16**, 9604 (2000).

⁹S. F. Chen, L. Y. Liu, and S. Y. Jiang, *Langmuir* **22**, 2418 (2006).

¹⁰K. Glasmastar, C. Larsson, F. Hook, and B. Kasemo, *J. Colloid Interface Sci.* **246**, 40 (2002).

¹¹M. Malmsten, *J. Colloid Interface Sci.* **168**, 247 (1994).

¹²E. Osterberg, K. Bergstrom, K. Holmberg, J. A. Riggs, J. M. Van Alstine, T. P. Schuman, N. L. Burns, and J. M. Harris, *Colloids Surf., A* **77**, 159 (1993).

¹³R. E. Marchant, S. Yuan, and G. Szakalasgratzl, *J. Biomater. Sci., Polym. Ed.* **6**, 549 (1994).

¹⁴S. L. McArthur, K. M. McLean, P. Kingshott, H. A. W. St. John, R. C. Chatelier, and H. J. Griesser, *Colloids Surf., B* **17**, 37 (2000).

¹⁵R. A. Frazier, G. Matthijs, M. C. Davies, C. J. Roberts, E. Schacht, and S. J. B. Tendler, *Biomaterials* **21**, 957 (2000).

¹⁶P. Kingshott, H. Thissen, and H. J. Griesser, *Biomaterials* **23**, 2043 (2002).

¹⁷J. L. Dalsin, L. J. Lin, S. Tosatti, J. Voros, M. Textor, and P. B. Messersmith, *Langmuir* **21**, 640 (2005).

¹⁸D. Lazos, S. Franzka, and M. Ulbricht, *Langmuir* **21**, 8774 (2005).

¹⁹O. H. Kwon, Y. C. Nho, K. D. Park, and Y. H. Kim, *J. Appl. Polym. Sci.* **71**, 631 (1999).

²⁰H. W. Ma, J. H. Hyun, P. Stiller, and A. Chilkoti, *Adv. Mater. (Weinheim, Ger.)* **16**, 338 (2004).

²¹R. J. Green, M. C. Davies, C. J. Roberts, and S. J. B. Tendler, *J. Biomed. Mater. Res.* **42**, 165 (1998).

²²M. Amiji and K. Park, *Biomaterials* **13**, 682 (1992).

²³L. M. Feller, S. Cerritelli, M. Textor, J. A. Hubbell, and S. G. P. Tosatti, *Macromolecules* **38**, 10503 (2005).

²⁴G. L. Kenausis *et al.*, *J. Phys. Chem. B* **104**, 3298 (2000).

²⁵C. FreijLarsson, T. Nylander, P. Jannasch, and B. Wesslen, *Biomaterials* **17**, 2199 (1996).

²⁶J. P. Bearinger, D. G. Castner, S. L. Golledge, A. Reznia, S. Hubchak, and K. E. Healy, *Langmuir* **13**, 5175 (1997).

²⁷T. A. Barber, S. L. Golledge, D. G. Castner, and K. E. Healy, *J. Biomed. Mater. Res. Part A* **64**, 38 (2003).

²⁸E. Ostuni, L. Yan, and G. M. Whitesides, *Colloids Surf., B* **15**, 3 (1999).

²⁹K. L. Prime and G. M. Whitesides, *J. Am. Chem. Soc.* **115**, 10714 (1993).

³⁰M. Mrksich, G. B. Sigal, and G. M. Whitesides, *Langmuir* **11**, 4383 (1995).

³¹K. Feldman, G. Hahner, N. D. Spencer, P. Harder, and M. Grunze, *J. Am. Chem. Soc.* **121**, 10134 (1999).

³²S. W. Lee and P. E. Laibinis, *Biomaterials* **19**, 1669 (1998).

³³N. Faucheux, R. Schweiss, K. Lutzow, C. Werner, and T. Groth, *Biomaterials* **25**, 2721 (2004).

³⁴S. Pasche, S. M. De Paul, J. Voros, N. D. Spencer, and M. Textor, *Langmuir* **19**, 9216 (2003).

³⁵N. P. Huang *et al.*, *Langmuir* **17**, 489 (2001).

³⁶R. Michel, S. Pasche, M. Textor, and D. G. Castner, *Langmuir* **21**, 12327 (2005).

³⁷M. S. Wagner, S. Pasche, D. G. Castner, and M. Textor, *Anal. Chem.* **76**, 1483 (2004).

³⁸N. P. Huang, J. Voros, S. M. De Paul, M. Textor, and N. D. Spencer, *Langmuir* **18**, 220 (2002).

³⁹G. L. Zhen, D. Falconnet, E. Kuennemann, J. Voros, N. D. Spencer, M. Textor, and S. Zurcher, *Adv. Funct. Mater.* **16**, 243 (2006).

⁴⁰S. VandeVondele, J. Voros, and J. A. Hubbell, *Biotechnol. Bioeng.* **82**, 784 (2003).

⁴¹S. Tosatti, S. M. De Paul, A. Askendal, S. VandeVondele, J. A. Hubbell, P. Tengvall, and M. Textor, *Biomaterials* **24**, 4949 (2003).

⁴²M. Schuler, G. R. Owen, D. W. Hamilton, M. De Wilde, M. Textor, D. M. Brunette, and S. G. P. Tosatti, *Biomaterials* **27**, 4003 (2006).

⁴³J. Dodd and T. M. Jessell, *Science* **242**, 692 (1988).

⁴⁴J. H. Lee, B. J. Jeong, and H. B. Lee, *J. Biomed. Mater. Res.* **34**, 105 (1997).

⁴⁵Y. Iwasaki, S. Sawada, N. Nakabayashi, G. Khang, H. B. Lee, and K. Ishihara, *Biomaterials* **20**, 2185 (1999).

⁴⁶T. Wu, K. Efimenko, and J. Genzer, *J. Am. Chem. Soc.* **124**, 9394 (2002).

⁴⁷B. Zhao, *Langmuir* **20**, 11748 (2004).

⁴⁸Y. Mei *et al.*, *Langmuir* **21**, 12309 (2005).

⁴⁹Y. Liu, V. Klep, B. Zdyrko, and I. Luzinov, *Langmuir* **21**, 11806 (2005).

- ⁵⁰M. R. Tomlinson and J. Genzer, *Macromolecules* **36**, 3449 (2003).
- ⁵¹C. Xu, T. Wu, C. M. Drain, J. D. Batteas, and K. L. Beers, *Macromolecules* **38**, 6 (2005).
- ⁵²L. Ionov, B. Zdyrko, A. Sidorenko, S. Minko, V. Klep, I. Luzinov, and M. Stamm, *Macromol. Rapid Commun.* **25**, 360 (2004).
- ⁵³K. Mougín, A. S. Ham, M. B. Lawrence, E. J. Fernandez, and A. C. Hillier, *Langmuir* **21**, 4809 (2005).
- ⁵⁴Y.-S. Lin and V. Hlady, *Colloids Surf., B* **2**, 481 (1994).
- ⁵⁵S. K. W. Dertinger, X. Y. Jiang, Z. Y. Li, V. N. Murthy, and G. M. Whitesides, *Proc. Natl. Acad. Sci. U.S.A.* **99**, 12542 (2002).
- ⁵⁶I. Caelen, A. Bernard, D. Juncker, B. Michel, H. Heinzelmänn, and E. Delamar, *Langmuir* **16**, 9125 (2000).
- ⁵⁷K. A. Fosser and R. G. Nuzzo, *Anal. Chem.* **75**, 5775 (2003).
- ⁵⁸S. T. Plummer, Q. Wang, P. W. Bohn, R. Stockton, and M. A. Schwartz, *Langmuir* **19**, 7528 (2003).
- ⁵⁹J. T. Smith, J. K. Tomfohr, M. C. Wells, T. P. Beebe, T. B. Kepler, and W. M. Reichert, *Langmuir* **20**, 8279 (2004).
- ⁶⁰C. L. Hypolite, T. L. McLernon, D. N. Adams, K. E. Chapman, C. B. Herbert, C. C. Huang, M. D. Distefano, and W. S. Hu, *Bioconjugate Chem.* **8**, 658 (1997).
- ⁶¹R. A. Venkateswar, D. W. Branch, and B. C. Wheeler, *Biomed. Microdevices* **2**, 255 (2000).
- ⁶²A. Y. Sankhe, B. D. Booth, N. J. Wiker, and S. M. Kilbey, *Langmuir* **21**, 5332 (2005).
- ⁶³L. Pardo, W. C. Wilson, and T. J. Boland, *Langmuir* **19**, 1462 (2003).
- ⁶⁴H. Baier and F. Bonhoeffer, *Science* **255**, 472 (1992).
- ⁶⁵S. Kramer, H. Xie, J. Gaff, J. R. Williamson, A. G. Tkachenko, N. Nouri, D. A. Feldheim, and D. L. Feldheim, *J. Am. Chem. Soc.* **126**, 5388 (2004).
- ⁶⁶S. Morgenthaler, S. Lee, S. Zürcher, and N. D. Spencer, *Langmuir* **19**, 10459 (2003).
- ⁶⁷P. Tengvall, in *Titanium in Medicine: Material Science, Surface Science, Engineering, Biological Response and Medical Applications*, edited by D. M. Brunette, P. Tengvall, M. Textor, and P. Thomsen (Springer, Heidelberg, 2000).
- ⁶⁸D. Falconnet, A. Koenig, T. Assi, and M. Textor, *Adv. Funct. Mater.* **14**, 749 (2004).
- ⁶⁹J. A. Defeijter, J. Benjamins, and F. A. Veer, *Biopolymers* **17**, 1759 (1978).